OPTICAL REVIEW Vol. 13, No. 3 (2006) 119–128

Invited Review Paper

Beam Combination using Stimulated Brillouin Scattering for the Ultimate High Power-Energy Laser System Operating at High Repetition Rate over 10 Hz for Laser Fusion Driver

Hong Jin KONG, Seong Ku LEE, Jin Woo YOON and Du Hyun BEAK

Department of Physics, KAIST, Guseong-dong, Yuseong-gu, Daejeon 305-701, Korea

(Received March 15, 2006; Accepted April 11, 2006)

After the laser was invented in 1960, a phase conjugation mirror has been respected to be the most fantastic one for the laser resonator composition because it can compensate any distortions of the laser beams occurred by the many inhomogenuities of the laser media and optical components. Among the many phase conjugation configurations, the stimulated Brillouin scattering phase conjugation mirror is the most simple one and many researchers have tried to utilize it to develop high power/energy laser systems. For realizing a high energy/power laser system the thermal problem is the most difficult to solve, and some researchers suggested a beam combination technique to reduce the thermal load of the big laser media to many small sized ones. To accomplish the beam combination using stimulated Brillouin scattering phase conjugation mirrors (SBS-PCMs), it is necessary to lock/control the phases of the SBS-PCMs. And some researchers have developed several ways for it, but they can lock the phases of a limited number of beams overlapped at the foci less than 5, or lock the phases by back-seeding technique but it loses the phase conjugation characteristics. For realization of the laser fusion driver, it is necessary to combine more than 10 or 100 beams. And the authors have developed recently a new phase controlling/locking technique which is isolated and independent totally from other beams and it can be applied to an unlimited number of beams in principle.

Key words: beam combination, laser fusion driver, phase control, stimulated Brillouin scattering

1. Introduction

Laser fusion energy will be realized only if the laser driver of the output energy of 10 MJ is required for fuel mass 10–20 mg.[1)] For laser fusion energy generation, this laser driver must operate with high repetition rate around 10 Hz, which is the most hard condition within the current laser technology,[2)] even if its gain will be increased very much with the help of the fast ignition technology.[3,4)] Usually we need hundreds of laser beams for laser fusion reaction for the uniform implosion of the target. For example, NIF employs 192 beams. We need to develop a laser fusion driver module of 50 KJ output energy operating at 10 Hz, when we assume 200 beams of the driver will be used for implosive heating. This high repetition rate high energy laser system is possible in the gas laser system, however, the gas laser system[5–8)] has its own problems such as energy instability and too big size of the laser system.[9,10)] In this aspect, the solid state laser system is more ideal than the gas laser system. However, this kind of highly repetitive solid state laser driver has not been realized yet because of the bad thermal properties of the solid laser media. (Solid state lasers such as NIF and GekkoXII can operate only with one shot per several hours.[11,12)])

To solve this thermal problem in solid state laser systems, many researchers have developed many types of the laser media with high thermal conductivity, laser diode (LD) pumping to reduce the thermal load, or using a beam combination technique to distribute the thermal load to many small pieces of the amplifiers.[13–18)] The sintered ceramic laser material[19–21)] is known as the most promising laser material for this purpose. LD pumping is also very effective to reduce the thermal load to the laser media. The "Mercury" laser system in LLNL[22,23)] has been successfully developed with the LD pumping to deliver 100 J at 10 Hz, but still the way to the several KJ laser system is long away to arrive. The new beam combination technique developed by authors is the most promising way to develop the real laser fusion driver in near future independent of the new ceramic laser media and LD pumping, because it can combine as many beams as we wish without any limitation. If we apply this new technique to combine 500 of the laser module of 100 J with 10 Hz using the beam combination technique, we can get 50 KJ output at 10 Hz simply. In this paper, we will introduce the conceptual design of the two beams combined 200 J with 10 Hz using this new technique.

The beam combination technique using stimulated Brillouin scattering phase conjugation mirror (SBS-PCM) has many advantages because it gives the phase conjugated wave[24)] that can compensate any optical distortions occurred in the amplifier chain for the good beam quality, and also can stabilize the beam pointing of the laser system if the cross symmetric SBS-PCM is applied for the amplifier system.[25)] For the beam combination technique, it is essential to control/lock the phases of the beams to be combined, so-called phase locking or phase controlling. For the phase locking of the beam combination with SBS-PCM, there are several different techniques developed such as the four wave mixing,[26–28)] the overlapping foci,[29–31)] the back-seeding by the Stokes wave,[32)] and the self-phase-controlling SBS-PCMs (SFC-SBS-PCMs).[14–16)] Among these locking techniques, SFC-SBS-PCM is applicable to the unlimited number of beams and the most simple so that this technique is the most promising way to the real laser fusion driver. The

four wave mixing technique has too much complicated optics to be applied to the many beams combination. The overlapping foci technique becomes very difficult to apply to many beams over 5, because the focal points will be highly distorted by the thermal effect due to the high energy at the focal spot and also it destroys the symmetry between the beams to give the unequal output characteristics. The back-seeding beam technique does not guarantee the phase conjugation of the SBS wave because the SBS wave follows the phase of the back-seeding beam not of the signal wave. H. J. Kong proposed the very new technique, so called self-phase-controlling of SBS-PCM using a single feedback mirror only, which can overcome all drawbacks of the previous techniques mentioned upper. This new technique is the most simple among the phase locking techniques developed previously, and furthermore it is possible not only to lock but also to control the phases of the SBS waves very accurately. Each beam's phase can be controlled totally independently just by changing the position of the mirror.

We propose a 200 J at 10 Hz laser system using this phase controlling system by two beam combination technique. The module of 100 J with 10 Hz laser system employ 30 discs of $60 \times 120 \times 5\,\mathrm{mm}^3$ ($W \times L \times t$) and flash lamp pumping. The flash lamps can be replaced by LDs simply changing the pumping cartridge in future if the budget allows. Two of these modules will be combined together to get 200 J output energy by the beam combination technique through the amplitude dividing technique or wave-front dividing technique.

The beam combination technique with SFC-SBS-PCM is easily scalable to unlimited number of beams so that the demonstration of 200 J with 10 Hz repetition rate is the most important step toward the future of the laser fusion driver.

2. Reflectivity of Stimulated Brillouin Scattering Phase Conjugation Mirrors

The SBS reflectivity is nearly equal to that of an ordinary mirror in the narrow band case wherein the pump bandwidth $\Delta\nu_p$ is smaller than the Brillouin line-width Γ, which corresponds to a steady state SBS.[33,34] However, from a practical point of view, many applications of a SBS phase conjugate mirror (PCM) would necessarily involve a broadband pumped SBS, which corresponds to a transient state SBS ($\Delta\nu_p > \Gamma$) because laser systems involving the use of the SBS-PCM have a broadband spectrum in general, in order to obtain high output power and short pulse widths.[35,36] Thus, it is particularly important to investigate the broadband pumped SBS. Several theoretical and experimental investigations have been reported on the SBS reflectivity using a broadband pump.[37–43]

For a broadband pump, the SBS reflectivity depends on the relationship between four parameters; the coherence length l_c, the characteristic interaction length z_o which is usually equal to the Rayleigh range, the mode spacing Ω_m, and the Brillouin line-width Γ.[37–43] We investigated the reflectivity of SBS-PCM when the coherence length is longer than the interaction length ($l_c > z_o$). In this regime, the SBS gain for the broadband pump is as high as that for the narrow band pump,[37–39] and hence, the SBS-PCM is most likely to apply to a laser system satisfying the condition $l_c > z_o$. It was reported the SBS gain was as same as that for a single longitudinal mode pump and is also independent of the mode structure if the pump laser mode spacing exceeds the Brillouin line-width ($\Omega_m > \Gamma$).[37] Besides, even if $\Omega_m < \Gamma$, off-resonant acoustic waves, which are generated by the beating between the pump laser mode and another Stokes mode, play an important role in enhancing the gain and the reflectivity.[40,41]

In all the previous works, however, the influence of the multi-mode pump, or in other words a broadband pump, was considered only for two or several longitudinal modes and low pump energy near the SBS threshold. We have found that SBS reflectivity is significantly affected by self-focusing in the case of the multi-mode pump with a large number of longitudinal modes. This is because the multi-mode pulse has the temporal intensity spikes, arising due to mode beating, which have enough power to induce nonlinear effects such as self-focusing and optical breakdown even near the SBS threshold. In this section, we investigate the characteristics of the SBS reflectivity by the multi-mode pump with large number of longitudinal modes over a wide range of energy, in contrast to the single-mode pump case. We have used four kinds of liquids with different nonlinear refractive index n_2 and the Brillouin line-width Γ.

The experimental setup for measuring the reflectivity of the SBS-PCMs is shown in Fig. 1. The pump laser used was a Q-switched Nd^{3+}:YAG laser (GCR-150-10, Spectra Physics) with a single-longitudinal mode injection seeder. This pump laser can be operated both in the single- and multi-mode. The laser line-width in the single-mode and the multi-mode cases were found to be $\sim 0.003\,\mathrm{cm}^{-1}$ (0.09 GHz) and $\sim 0.33\,\mathrm{cm}^{-1}$ (10 GHz), respectively. Thus, the line-width of the multi-mode case was much larger than the Brillouin line-width of the liquids used in this experiment, listed in Table 1,[34,44–46] implying that the multi-mode pump corresponds to a broadband pump and the high transient regime. The mode spacing Ω_m was $\sim 0.0061\,\mathrm{cm}^{-1}$ (183 MHz), and hence the number of modes of the multi-mode pump beam

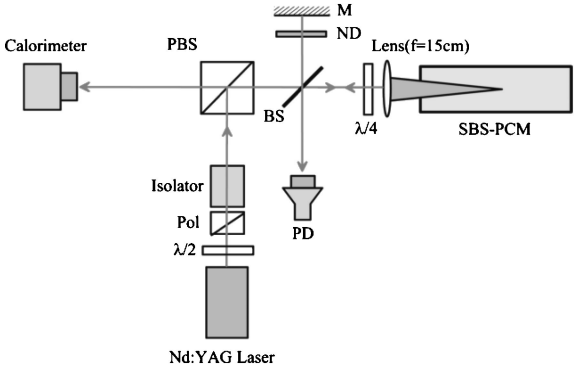

Fig. 1. Experimental setup for the measurement of the SBS reflectivity; $\lambda/2$, half wave plate; Pol, polarizer; M, mirror; ND, neutral density filter; $\lambda/4$, quarter wave plate; PBS, polarizing beam splitter; BS, beam splitter; PD, photodiode.

Table 1. Properties of the liquids, used for experiments at a wavelength of 1 μm.

Liquid	Γ (MHz)	g_B (cm/GW)	n_2 (10^{-22} m^2/V^2)	P_c (MW)	E_b (mJ)
Fluorinert FC-75	350	4.5–5	0.34	7.0	6
Carbon tetrachloride (CCl_4)	528	3.8	5.9	0.4	1.7
Acetone	119	15.8	8.6	0.28	1.5
Carbon disulfide (CS_2)	50	68	122	0.020	0.1

Γ, Brillouin line-width; g_B, steady state SBS gain; n_2, nonlinear refractive index; P_c, critical power for self-focusing (calculated); E_b, breakdown threshold energy (measured).

was as many as about 55. The pulse repetition rate was fixed at 10 Hz and the radius of the output beam was 4 mm. The focal length of the lens used was 15 cm.

This corresponds to a Rayleigh range z_o of ~0.62 mm. The coherence length l_c was found to be ~3.4 cm, which was measured directly using Michelson interferometer. Thus, the coherence length satisfies the condition $l_c \gg z_o$. The pulse width in both cases, single as well as multi-mode cases, was 6–8 ns (full width at half maximum). The spatial beam profiles in both cases were also almost same and nearly Gaussian. The pump energy was varied from 0 to 400 mJ by means of an attenuator, which consisted of a thin film polarizer and a half-wave plate. The fluctuation of the laser energy was less than 1% for both cases. A calorimeter (AstralTM AC2501, Scientech) was used to measure both the pump energy E_p and the reflected energy E_R, averaged for ~300 serial pulses. The SBS materials used in this experiment were Fluorinert FC-75, carbon tetrachloride (CCl_4), acetone, and carbon disulfide (CS_2). The SBS properties and the nonlinear refractive index n_2 of each liquid are shown in Table 1. They have different nonlinear refractive index n_2 ranging from 0.34 to 122 × 10^{-22} m^2/V^2. Besides, each liquid has different Brillouin line-width ranging from 50 to 528 MHz. The breakdown threshold E_b listed in Table 1 was measured when a bright spark appeared inside the SBS cell. Each liquid was purified with a syringe filter having 0.2 μm pore size to raise the breakdown threshold energy E_b. The length of a SBS cell was 30 cm. The cells were composed of a glass tube and windows, AR coated on one side only.

Figures 2 and 3 show the SBS reflectivity for both single- and multi-mode cases in CCl_4 and Fluorinert FC-75 as a function of the pump energy. It is seen that for both liquids, the peak values exceeding 90% can be obtained with the single-mode pump. The SBS reflectivity shows a typical nonlinear variation with the pump energy as in the case of steady state SBS. For the multi-mode pump, the SBS reflectivity is different for each of the liquids. The SBS gain for the multi-mode pump seems to be as high as that for the single-mode pump in both the liquids, considering that the SBS threshold for both the pump modes is approximately the same regardless of the liquids. However, in CCl_4, the peak reflectivity is 30% at most. FC-75 provides a peak reflectivity over 65% but the reflectivity decreases as the pump energy increases. Especially, the SBS reflectivity in CCl_4 is slightly higher for the multi-mode pump than that for the single-mode pump near the SBS threshold of the single-mode case although, in general, the single-mode pump has

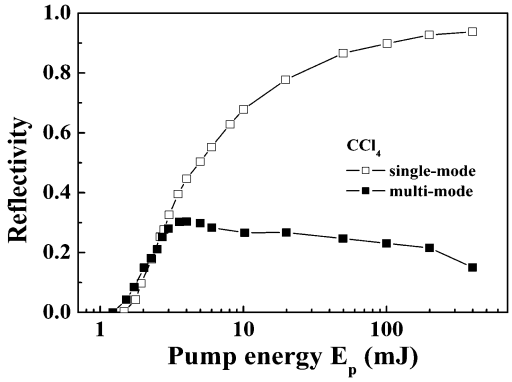

Fig. 2. SBS reflectivity vs pump energy for CCl_4 as active medium and for laser radiation in the single-mode and multi-mode cases.

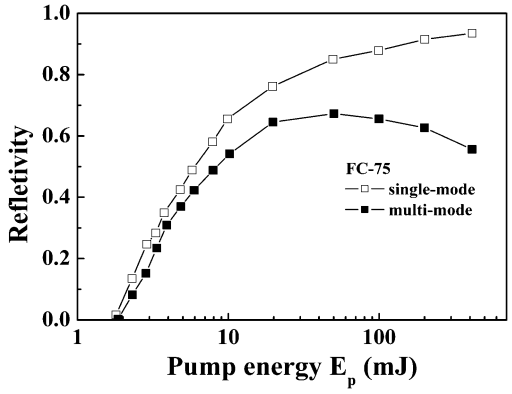

Fig. 3. SBS reflectivity vs pump energy for FC-75 as active medium and for laser radiation in the single-mode and multi-mode cases.

a higher SBS gain.[47] However, for FC-75 the behavior is exactly opposite. Note that both CCl_4 and FC-75 have very similar SBS properties such as the SBS gain and Brillouin line-width (see Table 1), which results in similar reflectivity for both liquids for the single-mode pump case. Several factors appear to contribute to the SBS for the multi-mode pump case. We interpret the SBS reflectivity for the multi-mode pump in terms of the temporal intensity spikes of the multi-mode pulse, which is absent in the single-mode pulse. This is because the intensity spikes, created by beating between a large number of longitudinal modes have enough power to induce the nonlinear effects such as self-focusing and the optical breakdown. In our experiments, the multi-

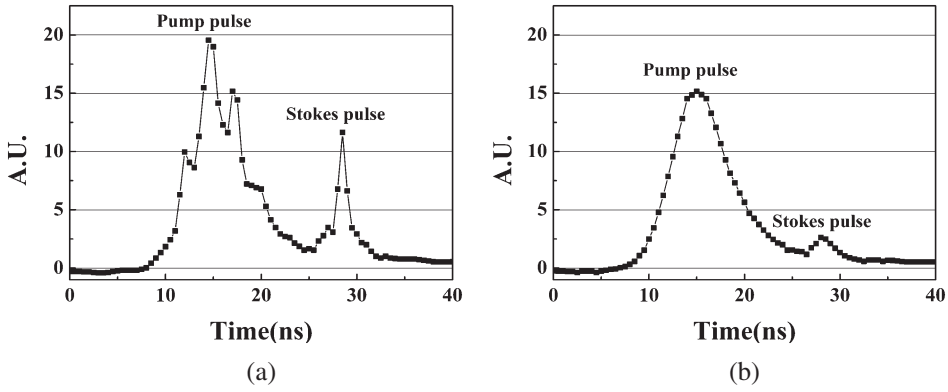

Fig. 4. Pump and reflected pulse shapes in (a) multi-mode and (b) single-mode case at $E_p \sim 1.5$ mJ in CCl_4.

mode pulse is composed of 55 longitudinal modes, implying that the peak intensity of the multi-mode pump can be 55 times higher than that of the single-mode pump if perfect mode locking is achieved.

First of all, the self-focusing due to the intensity spikes is likely to lead to anomalously high reflectivity of the multi-mode pump near the SBS threshold in CCl_4. The critical power of the self-focusing is given by

$$P_c = \pi \varepsilon_o c^3/(n_2 \omega^2), \quad (1)$$

where ε_o and c are the permittivity of vacuum and the speed of light, respectively.[48] Using eq. (1), the critical power P_c for CCl_4 and FC-75 are 0.4 and 7.0 MW, respectively; the nonlinear refractive index n_2 is listed in Table 1. Compared to the SBS threshold (~5% energy reflection) for the single-mode pump case for CCl_4, which is approximately 1.8 mJ (0.26 MW), the critical power of 0.4 MW is slightly large. However, we believe that it is possible for the multi-mode pulse to induce the temporal small scale self-focusing in CCl_4 below the SBS threshold because the intensity spikes can have high peak power exceeding the critical power P_c. Figure 4 represents the temporal pulse shapes of the pump and Stokes pulse with different energy scales for both pump types, when the pump beam with $E_p \sim 1.5$ mJ was focused into a CCl_4 cell. This was measured using a fast photodiode (Newport 818-BB-30) connected to a Hewlett Packard 54542C digital oscilloscope. As expected, the multi-mode pulse has large intensity spikes, which do not show up in the single-mode pulse. In addition, it is well known that self-focusing is dependent on the power and not the energy of the light. Thus, the multi-mode pulse can induce self-focusing in CCl_4 due to the high intensity spikes even at powers lower than SBS threshold. Self-focusing leads to increase in the intensity of the pump beam in the focal region and hence, can reduce the SBS threshold energy, assuming the steady state SBS threshold relationship $I_{th} g_B l = 25-30$ to hold to a good approximation, where I_{th}, g_B, and l are the SBS threshold intensity, the SBS gain, and the interaction length, respectively.[33] Consequently, self-focusing results in lower SBS threshold and slightly higher reflectivity near the SBS threshold in the CCl_4 as shown in Fig. 2. We note that backward stimulated Raman scattering (SRS) was not observed in this low energy regime up to 10 mJ. On the other hand, the SBS reflectivity in the FC-75 is not affected by the self-focusing near the SBS threshold because the critical power for FC-75 is approximately 18 times larger than for CCl_4. Consequently, the SBS reflectivity for the multi-mode pump is lower than that for the single-mode pump near the SBS threshold. The self-focusing seems to be deleterious for SBS since it can enhance optical breakdown. It can be certified from the experimental results that the optical breakdown in CCl_4 starts at $E_p \sim 1.7$ mJ while it began at ~6 mJ in FC-75, as listed in Table 1. We have observed that the breakdown appears around the focal spot near breakdown threshold and it becomes severe and results in a filament consisting of bright sparks, as the pump energy increases. This breakdown disturbs the creation of the acoustic phonon. Therefore, for the multi-mode pump, FC-75, which has relatively small n_2 provides higher SBS reflectivity than CCl_4 at high pump energies. On the other hand, for the single-mode pump, reflectivity of both the liquids was almost the same because no optical breakdown occurred up to the pump energy of 400 mJ.

In addition to the breakdown due to self-focusing, an intensity spike can easily generate optical breakdown by itself because it has a very steep rising edge. It is well known that for efficient SBS to occur, temporal fluctuations in the pump must be slow compared to the acoustic phonon lifetime. If the temporal fluctuations are fast relative to the acoustic phonon lifetime, the acoustic waves do not get the time to build up. The intensity spikes with the steep rising edge and energies exceeding the breakdown threshold can, therefore, reach the focal area without losing their energy by the backward reflection. Hence, they can generate optical breakdown and reduce the SBS reflectivity even at low energy. For the single-mode case, the region of SBS reflection moves fast, along with the SBS pulse, opposite to the pump pulse and the pump pulse is reflected well from a region before the focal area wherein the optical intensity is too small to induce the optical breakdown.[49] Therefore, optical breakdown is not generated for the single-mode pump even with the strong pump energy.

Figure 5 shows the SBS reflectivity for acetone. It is shown that the multi-mode pump provides higher reflectivity

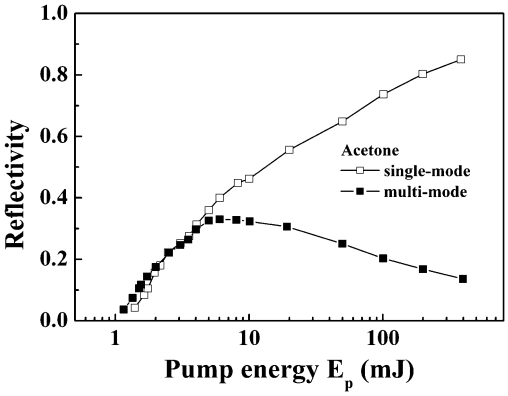

Fig. 5. SBS reflectivity vs pump energy for acetone as active medium and for laser radiation in the single-mode and multi-mode cases.

than the single-mode pump near the SBS threshold, which is very similar to the results in the case of CCl_4. The backward SRS was not observed in this low energy regime. From Table 1, acetone has approximately the same nonlinear refractive index as CCl_4. From the above results, it is clear once again that SBS reflectivity by the multi-mode pump, with a large number of longitudinal modes, is significantly affected by self-focusing due to the high intensity spikes. The reflectivity for the multi-mode pump increases with energy up to 6 mJ and decreases strongly thereafter because the breakdown becomes severe, whereas the single-mode pump provides monotonically increasing reflectivity.

Finally, Fig. 6 shows the measured reflectivity of CS_2. Of all the four liquids examined, CS_2 has the lowest SBS threshold energy ~0.3 mJ and the highest reflectivity ~95% in the single-mode pump case because it has the highest steady state SBS gain (Table 1). On the contrary, the SBS reflectivity by the multi-mode pump is the lowest and almost zero in the entire region. The critical power ~20 kW for self-focusing is about half of the SBS threshold ~40 kW. Besides, CS_2 has the longest acoustic lifetime of 6 ns among the liquids used,[45] which is comparable to the pulse-width of the pump beam. As already mentioned, if the temporal fluctuations of the pump pulse are fast relative to the acoustic phonon lifetime, the acoustic waves do not get the time to build up. As a result, CS_2 has very low breakdown threshold ~0.1 mJ lower than the SBS threshold, which can account for the almost zero reflectivity observed. We have observed that optical breakdown results in a filament in the case of very weak pump energy close to the SBS threshold. It is noted that SRS may be also responsible for the low reflectivity. CS_2 has a high SRS gain. The SRS process has a very short response time of 10^{-11} s, implying that it can respond better than SBS process to the intensity spikes of the multimode pulse.[50]

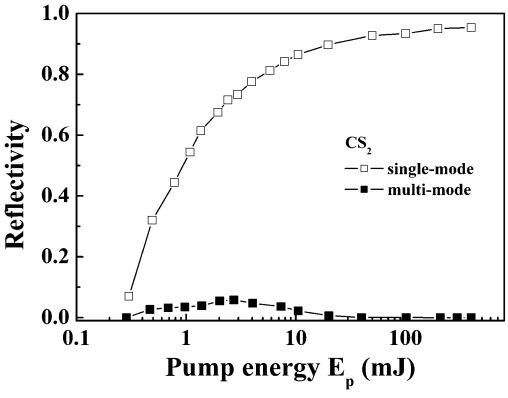

Fig. 6. SBS reflectivity vs pump energy for CS_2 as active medium and for laser radiation in the single-mode and multi-mode cases.

We have investigated SBS reflectivity by a multi-mode pump with a large number of longitudinal modes, as compared with the single-mode pump case. We have used four kinds of liquids with different nonlinear refractive index and Brillouin line-width. It is found that in all the cases except CS_2, the SBS reflectivity by the multi-mode pump increases rapidly and then decreases slowly as the pump energy increases although the SBS gain is as high as that for the single-mode pump. For the case of CS_2, the reflectivity is generally very low although the nature of variation is similar to that for the other liquids. On the contrary, the single-mode pump provides a stable and high reflectivity. This is because a multi-mode pulse, consisting of a large number of longitudinal modes, has high intensity spikes created by mode beating, which have enough power to induce optical breakdown and nonlinear effects such as self-focusing. Especially, it is found that the SBS reflectivity using a multi-mode pump is significantly affected by self-focusing because it can not only enhance SBS even at powers lower than the SBS threshold, but also suppress SBS by generating strong optical breakdown at high pump energy.

3. Self-Generated Density Modulation Method for Phase Controlling—Wave-Front Dividing

The experimental setup is shown schematically in Fig. 7(a). A 1064 nm Nd:YAG oscillator with a bandwidth of ~120 MHz was used for the pump. The pulse width was 7–8 ns and the repetition rate was 10 Hz. The output from an oscillator passes through a 2× cylindrical telescope and is divided into two beams by a prism, which has high reflection coating for 45 deg incident angle. Both beams then pass through separate wedges and are focused into each SBS-PCM. The wedge reflects a part of the backward Stokes beam, which is overlapped with that of the other Stokes beam onto a CCD camera to get an interference pattern of them. For controlling the phase by the self-generated density modulation, the pump pulse focused into the SBS-PCM is reflected partially by the uncoated concave mirror (~4% reflection), so that a standing wave is built up, especially at the focal area by the interference between the leading edge and the remaining part of the pump pulse. The leading edge reflected by the uncoated concave mirrors is so weak that the density modulation induced by the standing wave due to electrostriction is also weak and does not disturb the acoustic wave generated by coupling the pump and the Stokes beam. We used Fluorinert FC-75 as a SBS medium.[34] The length of a SBS cell was 50 cm.

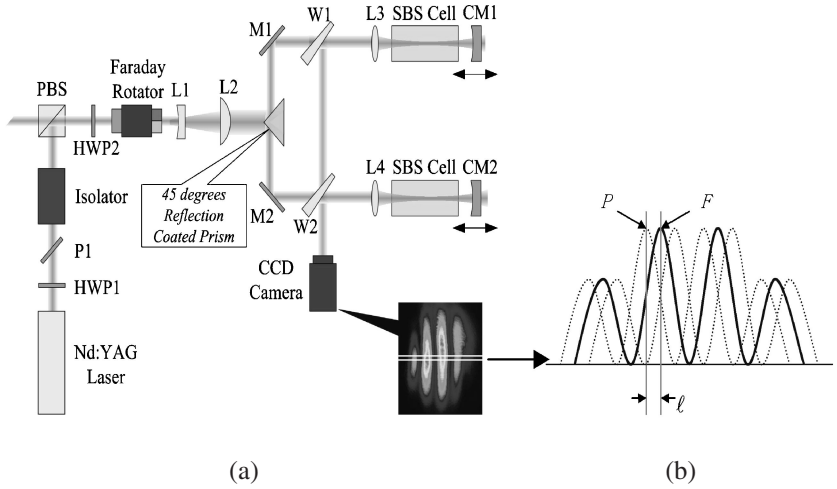

Fig. 7. (a) Experimental setup for the phase locking of two laser beams: M1 and M2, mirrors; W1 and W2, wedges; L1 and L2, cylindrical lenses: L3 and L4, focusing lenses, CM1 and CM2, concave mirrors; HWP1 and HWP2, half wave-plates; P1, polarizer; PBS, polarizing beam splitter. (b) Measurement of the relative phase difference δ between two beams. The fluctuation of the relative phase difference is expressed as $2\pi\lambda/T$, where T is a spatial period of the interference pattern.

The diagnostics for the phase control of the Stokes beams is straightforward. The interference pattern acquired by the CCD camera yields the relative phase difference $\delta = \Phi_1 - \Phi_2$ between the laser beams incident on the CCD, where Φ_1 and Φ_2 denote the phases of two laser beams, respectively. Therefore, we can quantitatively analyze the degree of the phase controlling by measuring the movement of the peaks. In every interference pattern, one horizontal line is selected as shown in Fig. 7(b). A peak position P is then determined from the selected line. Since the relative phase difference δ between two beams fluctuates, the peak position P also moves to the left or right with respect to some fixed point F. When λ is the distance between F and P, the relative phase difference δ can be expressed as $2\pi\lambda/T$, where T is a spatial period of the interference pattern.

Figure 8 shows the experimental schematic and results for the unlocked case when the focal length of the focused lenses was 25 cm and energy of each incident beam was ~9 mJ. Each point in Fig. 8(c) represents one of 160 laser pulses. As naturally expected, δ has random values and the standard deviation (SD) is $\sim 0.295\lambda$. This indicates that the phases of two backward beams are independent and are not fixed. Figure 8(b) shows the intensity profile of the 160 horizontal lines selected from each interference pattern. The profile also represents the random fluctuation. Figure 9(a) shows the first experimental schematic for controlling the phase of the SBS wave by generating the weak density modulation. The pump beam was reflected by the uncoated concave mirror with $R = 300$ mm and then injected into SBS-PCM. The relative phase difference δ is shown in Fig. 9(c). The energy of each incident beam was 13 mJ and 203 laser pulses were examined. The SD is $\sim 0.165\lambda$. Moreover, 88% of the data points is contained within the range of $\pm 0.25\lambda$ ($\pm 90^\circ$). This result gives a demonstration that the self-generated density modulation can make the phase of the backward SBS wave fixed. In addition, we observed that the phase of the SBS wave was varied by the

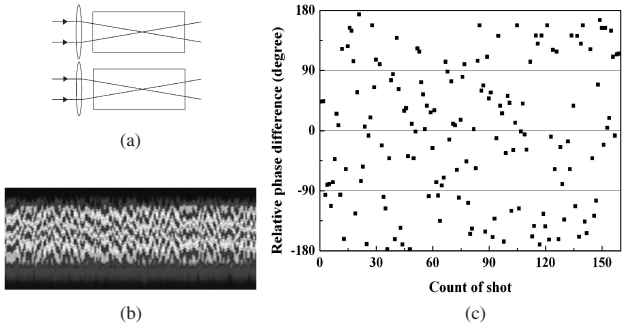

Fig. 8. (a) Schematic of the unlocked case. (b) Intensity profile of horizontal lines selected from 160 interference patterns. (c) Relative phase difference between two beams for 160 laser pulses.

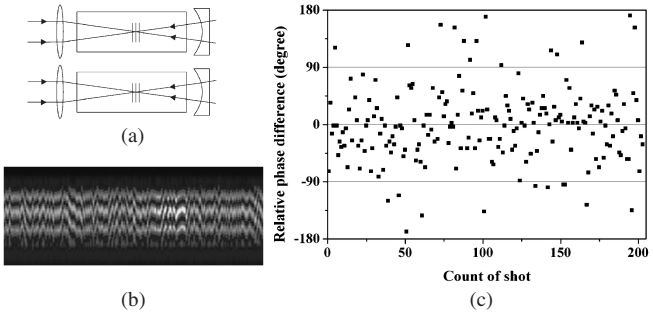

Fig. 9. (a) Weak density modulation by a concentric type. (b) Intensity profile of horizontal lines selected from 203 interference patterns. (c) Relative phase difference between two beams for 203 laser pulses.

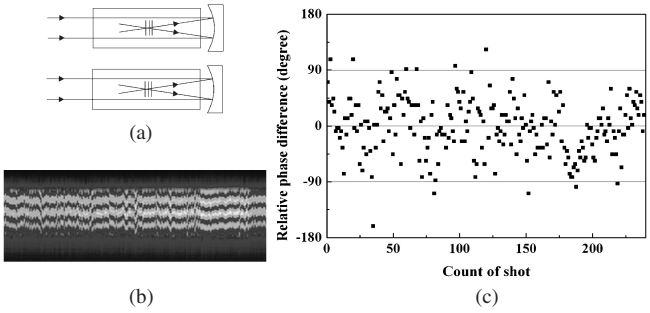

Fig. 10. (a) Weak density modulation by backward focusing. (b) Intensity profile of horizontal lines selected from 238 interference patterns. (c) Relative phase difference between two beams for 238 laser pulses.

precise movement of the concave mirror where a PZT was attached. As the mirror position was changed by PZT, the interference pattern moved slowly into one direction although the fluctuations existed. This implies that we can control the phase of the SBS waves freely and get rid of the intensity spikes of the beam combination laser by making the relative phase be zero. We note that this method can be applied to the beam combination laser composed of a large number of laser beams although the experiment has been carried out for just two laser beams. This can be justified if we consider the two laser beams in the experiment as a set of arbitrary two laser beams among the large number of a laser system statistically, because our method corresponds to absolutely uncoupled beams. The optical path length between the focal point and the uncoated concave mirror is longer than 30 cm in this setup, considering the radius of curvature of the uncoated concave mirror ($R = 30$ cm) and the refractive index of FC-75 ($n = 1.268$). Thus, considering a round-trip, the SBS may be generated from the acoustic noise before the density modulation is induced because the density modulation is generated only after more than 2 ns after the pump laser pulse reaches the focal point. This may increase the fluctuation of the relative phase difference.

To reduce the fluctuation, we repeated the measurements for another scheme as shown in Fig. 10(a), where the pump beams was backward focused by a concave mirror with $R = 50$ cm and $>99\%$ reflectivity at the laser wavelength. In this case, the delay time to induce the density modulation is almost zero. However, the contrast of the standing wave which is expressed as $(I_{\max} - I_{\min})/(I_{\max} + I_{\min})$ is so small that the density modulation is not quite distinct as compared to the previous scheme because the focused leading edge of the pump pulse encounters a part of the unfocused pump pulse. The experimental result is shown in Fig. 10(c) when the incident energy was 8 mJ and 238 laser pulses were examined. The SD is $\sim 0.135\lambda$. Furthermore, 96% of the data points are contained in the range of $\pm 0.25\lambda$. Therefore, it has been shown that the degree of the phase controlling can be very much improved. The intensity profile of the horizontal lines in Fig. 10(b) also manifests the improved result.

4. Self-Generated Density Modulation Method for Phase Controlling—Amplitude Dividing

The experimental setup is shown schematically in Fig. 11. Figure 12(a) shows the Fabry–Perot interferograms for the pump laser (left) and the SBS return from the SBS-PCM with the phase control technique (right). We have used the Fabry–Perot interferometer with the free spectral range of 5 GHz. The interferograms show that the backward SBS wave is reflected only by the acoustic wave, but the Bragg scattering by the density modulation is not generated because there is no overlapping between two interferograms, considering that the Brillouin frequency shift is 1.34 GHz for FC-75.[34] Figure 12(b) shows the Fabry–Perot interferograms for the SBS return from the SBS-PCM with no phase control technique (left) and the SBS return from the SBS-PCM with the phase control technique (right). The results also demonstrate that the SBS wave is reflected only by the acoustic wave.

The experimental investigation carried out for the cases

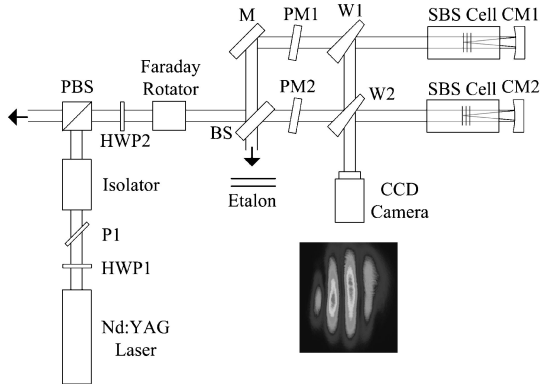

Fig. 11. Experimental setup for measuring the relative phase difference; HWP1 and HWP2, half wave plates; BS, beam splitter; M, mirror; PM1 and PM2, partial reflection mirrors; W1 and W2, wedges; P1, polarizer; PBS, polarization beam splitter; CM1 and CM2, concave mirrors.

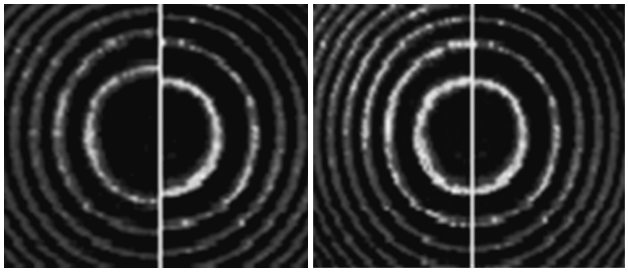

Fig. 12. Fabry–Perot interferograms. (a) The spectra of the pump laser (left) and the SBS wave reflected from the SBS-PCM with the phase control technique (right). (b) The spectra of the SBS wave reflected from the SBS-PCM with no phase control technique (left) and that with the phase control technique (right). The free spectral range of the interferometer is 5 GHz.

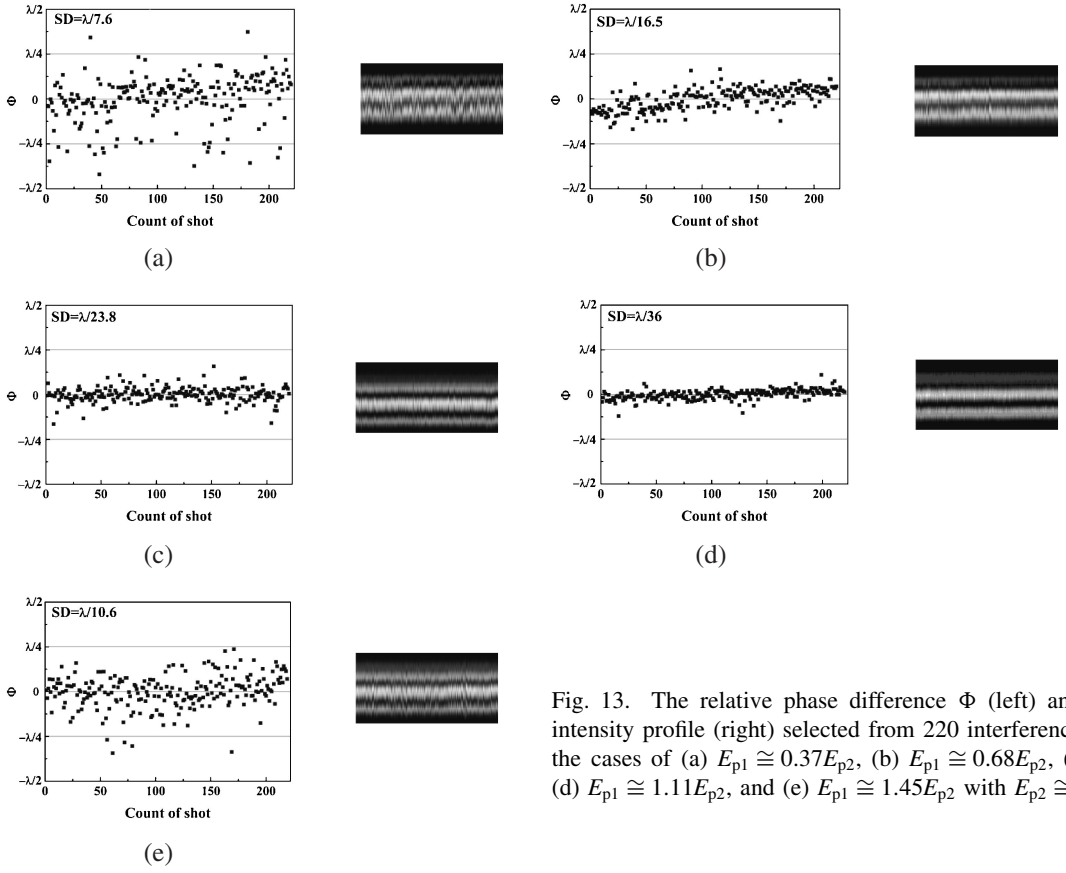

Fig. 13. The relative phase difference Φ (left) and the mosaic intensity profile (right) selected from 220 interference patterns for the cases of (a) $E_{p1} \cong 0.37E_{p2}$, (b) $E_{p1} \cong 0.68E_{p2}$, (c) $E_{p1} \cong E_{p2}$, (d) $E_{p1} \cong 1.11E_{p2}$, and (e) $E_{p1} \cong 1.45E_{p2}$ with $E_{p2} \cong 10\,\mathrm{mJ}$.

of $E_{p1} \cong 0.37E_{p2}$, $E_{p1} \cong 0.68E_{p2}$, $E_{p1} \cong E_{p2}$, $E_{p1} \cong 1.11E_{p2}$, and $E_{p1} \cong 1.45E_{p2}$ with $E_{p2} \cong 10\,\mathrm{mJ}$, where E_{p1} and E_{p2} denote the energies of two sub-pump-beams, in order to investigate the pump energy dependency of the phase of the SBS wave. We have measured the relative phase difference Φ for measuring the degree of the phase stabilization. Figure 13 shows the experimental results. Each point in Figs. 13(a), 13(b), 13(c), 13(d), and 13(e) represents one of 220 laser pulses. The SDs of the relative phase difference for the cases of $E_{p1} \cong 0.37E_{p2}$, $E_{p1} \cong 0.68E_{p2}$, $E_{p1} \cong E_{p2}$, $E_{p1} \cong 1.11E_{p2}$, and $E_{p1} \cong 1.45E_{p2}$ are $\lambda/7.6$, $\lambda/16.5$, $\lambda/36$, $\lambda/23.8$, and $\lambda/10.6$, respectively. From these results, it can be noted that the relative phase difference Φ becomes more stabilized as E_{p1} approaches E_{p2} and Φ is mostly stabilized for the case of $E_{p1} \cong E_{p2} \cong 10\,\mathrm{mJ}$. In Fig. 13, the right figures show the mosaic intensity profiles composed of 220 lines selected from each interference pattern. The intensity profile, as shown in Fig. 13(c) also represents that Φ is remarkably stabilized for the case of $E_{p1} \cong E_{p2} \cong 10\,\mathrm{mJ}$. These results show that the phase of the SBS wave depends on the pump energy under the self-generated density modulation.

Let us assume that the main pump energy is given by $E_p = E_0 + \Delta E$, where E_0 is the average pump energy and ΔE is the variation in the pump energy caused by the energy fluctuation of the oscillator output. The energies of two divided pump beams can be written as $E_{p1} = r(E_0 + \Delta E)$ and $E_{p2} = (1 - r)(E_0 + \Delta E)$, where r is the division ratio of the beam splitter. Thus, the energy change of two divided pump beams can be given by $\Delta E_{p1} = r\Delta E$ and $\Delta E_{p2} = (1 - r)\Delta E$. Because the value of ΔE changes randomly, the energies of two divided pump beams also change for every shot to shot, which can induce the fluctuation of the relative phase difference because the phase of the SBS wave depends on the pump energy for this phase controlling scheme. However, if r is equal to 0.5, the effect of the energy fluctuation of the main beam on the relative phase difference will vanish for $E_{p1} = E_{p2}$. The experimental results also show that the relative phase difference Φ is mostly stabilized for the case of $r \sim 0.5$. Thus, the balancing the pump energies can easily make the relative phase difference be stabilized even if the energy fluctuation of the oscillator output exists. In addition, compared with the wave-front dividing cases,[14,16] in which the division ratio r is fluctuated randomly due to the beam pointing effect of the oscillator, it is seen that the fluctuation of the relative phase difference for the amplitude dividing case is considerably reduced. Consequently, we have shown that it is possible to stabilize the relative phase difference between the SBS waves by inducing the self-generated density modulation, provided that the pump energies are balanced, and the phase of the SBS wave significantly depends on the pump energy under the self-generated density modulation.

5. Design of the Laser Fusion Driver

The laser fusion driver is proposed in the Figs. 14 and 15 which are the wave-front and amplitude dividing techniques. All of the amplifier units are the same to operate at repetition

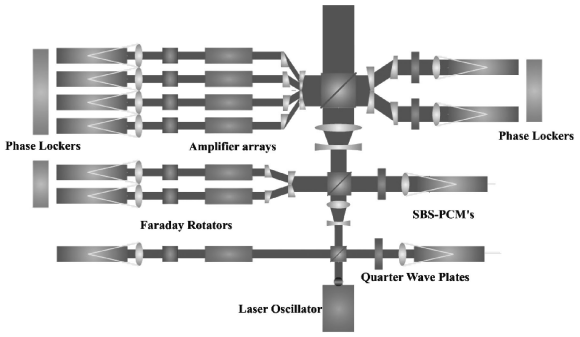

Fig. 14. Scalable beam combination system for laser fusion driver. All of the amplifier units are same to operate with high repetition rate over 10 Hz and the whole system can operate at the same repetition rate as the unit amplifier.

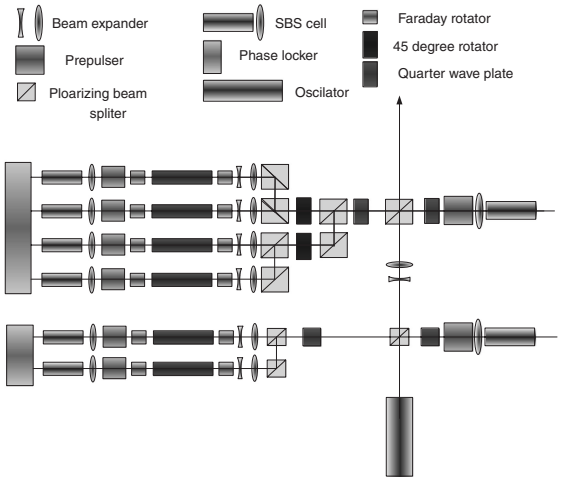

Fig. 15. Scalable beam combination with the amplitude dividing. All of the amplifier units are same to operate with high repetition rate over 10 Hz and the whole system can operate at the same repetition rate as the unit amplifier.

rate over 10 Hz and they can be pumped by flash lamps or LDs. Each amplifier unit is expected to produce 100 J per pulse at 10 Hz repetition rate. For the wave-front dividing scheme, the tolerance of the phase controlling might be less than $\lambda/4$ while it should be less than $\lambda/30$ for the amplitude dividing to get the energy fluctuation less than 3%. For the wave-front dividing scheme, the beam pointing should be very stable because its instability is directly related to the phase fluctuation. For amplitude dividing, the beam pointing is less sensitive than the wave-front dividing case but the combined energy fluctuate much more than the wave-front dividing case. Fortunately, the theoretical simulation by the authors shows that the phase fluctuation decreases as the pumping energy increases.[51] It helps to increase the accuracy of the phase controlling by increasing the amplifier output energy, which is very good news for developing high energy lasers. Figure 16 shows the theoretical simulation for the energy tolerance depending on the pumping energy for getting the phase accuracy less than $\lambda/100$. For example, the pumping energy over 1 and 10 J gives the phase fluctuations

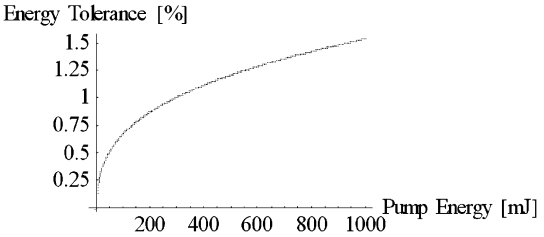

Fig. 16. The energy tolerance vs pumping energy for phase accuracy less than $\lambda/100$ (theory). Energy fluctuation tolerance for phase accuracy less than $\lambda/100$ is 3.4% for 10 J pump energy; 2.7% for 5 J pump energy; 1.5% for 1 J pump energy; 1.2% for 500 mJ pump energy; 0.67% for 100 mJ pump energy; 0.22% for 10 mJ pump energy; 0.11% for 5 mJ pump energy.

much less than $\lambda/100$ for the pumping energy fluctuations 1.5 and 3.4%, respectively.

The reflectivity and efficiency of the SBS wave depends strongly on the pumping laser's mode, and it is reported in the recent publication of the authors.[52] The single longitudinal mode regime of the pumping laser shows much better features than the multi-mode one.

The waveform of the SBS wave is known as distorted by the SBS intrinsic process. We proposed and demonstrated the preservation of its pulse shape by the "*pre-pulse technique*".[18]

6. Future Work

The SBS medium shows the thermal density fluctuation due to the temperature changes in the medium, and it changes the phases of the laser beam resulting in the phase fluctuations of the beams. This can be compensated by feedback the output signal to the PZT attached to the feedback mirror for compensating the fluctuation. This work has been finished successfully and it will be published soon.

7. Conclusions

The phase control of SBS wave by "the self-generated density phase modulation" has been proposed and demonstrated successfully in these experiments, and it has been tested by the theoretical simulation developed newly in this laboratory. We have found that the phase of the SBS wave is determined by the pumping energy and the nodal points of the standing wave generated by the feedback mirror for the self-generated density phase modulation. This new phase controlling technique can control the phase of SBS wave as we want very accurately and also its tolerance increases as the pumping energy increases, which is very good for realization of a laser fusion driver. We have proposed and demonstrated the preservation of its pulse shape by pre-pulse technique. We have proposed two types of the beam combination, a wave-front dividing and an amplitude dividing technique looks like better than the other. But if we have a very stable beam pointing laser sources, the wave-front dividing might be easier to for the beam combination. The laser fusion driver can be realized by this beam combination technique by SBS-PCMs using the newly developed phase controlling technique.

Acknowledgment

This work was supported by the IAEA, Austria, contract No. 11636/R2, and the Korean Ministry of Commerce, Industry and Energy within the project, "Development of Precision-Machining Technology using Advanced Lasers".

References

1) S. Atzeni and J. Meyer-Ter-Vehn: *The Physics of Inertial Fusion* (Oxford University Press, 2004) p. 416.
2) S. Nakai and K. Mima: Rep. Prog. Phys. **67** (2004) 321.
3) R. Kodama *et al.*: Nature **412** (2001) 798.
4) R. Kodama *et al.*: Nature **418** (2002) 933.
5) J. D. Sethian *et al.*: Proc. IEEE **92** (2004) 1043.
6) I. Okuda, E. Takahashi, I. Matsushima, Y. Matsumoto, S. Kato and Y. Owadano: Jpn. J. Appl. Phys. **40** (2001) 1152.
7) M. Watanabe, K. Hata, T. Adachi, R. Nodomi and S. Watanabe: Opt. Lett. **15** (1990) 845.
8) M. C. Myers, J. D. Sethian, J. L. Giuliani, R. Lehmberg, P. Kepple, M. F. Wolford, F. Hegeler, M. Friedman, T. C. Jones, S. B. Swanekamp, D. Weidenheimer and D. Rose: Nucl. Fusion **44** (2004) 247.
9) T. Matsunaga, T. Enami, K. Kakizaki, T. Saito, S. Tanaka, H. Nakarai, T. Inoue and T. Igarashi: Proc. SPIE **4346** (2001) 1617.
10) J. F. Ready: *Industrial Applications of Lasers* (Academic Press, 1997) Chap. 3.
11) J. D. Kilkenny, E. M. Campbell, J. D. Lindl, G. B. Logan, W. R. Meier, L. J. Perkins, J. A. Paisner, M. H. Key, H. T. Powell, R. L. McCrory and W. Seka: Trans. R. Soc. London, Ser. A **357** (1999) 533.
12) A. Schaper: Sci. Global Security **2** (1991) 279.
13) H. J. Kong, J. Y. Lee, Y. S. Shin, J. O. Byun, H. S. Park and H. Kim: Opt. Rev. **4** (1997) 277.
14) H. J. Kong, S. K. Lee and D. W. Lee: Laser Particle Beams **23** (2005) 55.
15) H. J. Kong, S. K. Lee and D. W. Lee: Laser Particle Beams **23** (2005) 107.
16) H. J. Kong, S. K. Lee, D. W. Lee and H. Guo: Appl. Phys. Lett. **86** (2005) 051111.
17) S. K. Lee, H. J. Kong and H. Guo: Appl. Phys. Lett. **87** (2005) 161109.
18) H. J. Kong, D. H. Beak, D. W. Lee and S. K. Lee: Opt. Lett. **30** (2005) 3401.
19) J. Kong, D. Y. Tang, J. Lu, K. Ueda, H. Yagi and T. Yanagitani: Opt. Commun. **237** (2004) 165.
20) J. Lu, T. Murai, K. Takaichi, T. Uematsu, K. Misawa, M. Prabhu, J. Xu and K. Ueda: Appl. Phys. Lett. **78** (2001) 3586.
21) J. Lu, J. Lu, T. Murai, K. Takaichi, T. Uematsu, J. Xu, K. Ueda, H. Yagi, T. Yanagitani and A. A. Kaminskii: Opt. Lett. **27** (2002) 1120.
22) S. A. Payne *et al.*: J. Fusion Energy **17** (1998) 213.
23) J. D. Sethian *et al.*: Nucl. Fusion **43** (2003) 1693.
24) B. Ya. Zel'dovich, V. I. Popovichev, V. V. Ragul'skii and F. S. Faizullov: Sov. Phys. JETP Lett. **15** (1972) 109.
25) H. J. Kong, S. K. Lee, J. J. Kim, Y. G. Kang and H. Kim: Chin. J. Lasers B **10** (2001) Suppl., p. I5.
26) N. F. Andreev, E. A. Khazanov, S. V. Kuznetsov, G. A. Pasmanik, E. I. Shklovsky and V. S. Sidorin: IEEE J. Quantum Electron. **27** (1991) 135.
27) M. W. Bowers and R. W. Boyd: IEEE J. Quantum Electron. **34** (1998) 634.
28) K. D. Ridley and A. M. Scott: J. Opt. Soc. Am. B **13** (1996) 900.
29) D. A. Rockwell and C. R. Giuliano: Opt. Lett. **11** (1986) 147.
30) H. Becht: J. Opt. Soc. Am. B **15** (1998) 1678.
31) R. H. Moyer, M. Valley and M. C. Cimolino: J. Opt. Soc. Am. B **5** (1988) 2473.
32) T. R. Loree, D. E. Watkins, T. M. Johnson, N. A. Kurnit and R. A. Fisher: Opt. Lett. **12** (1987) 178.
33) R. W. Boyd: *Nonlinear Optics* (Academic Press, 1992) Chap. 8.
34) H. Yoshida, V. Kmetik, H. Fujita, M. Nakatsuka, T. Yamanaka and K. Yoshida: Appl. Opt. **36** (1997) 3739.
35) A. A. Shilov, G. A. Pasmanik and O. V. Kulagin: Opt. Lett. **26** (2001) 1565.
36) B. Králiková, J. Skála, P. Straka and H. Turčičová: Appl. Phys. Lett. **77** (2000) 627.
37) P. Narum, M. D. Skeldon and R. W. Boyd: IEEE J. Quantum Electron. **22** (1986) 2161.
38) Yu. E. D'yakov: JETP Lett. **11** (1970) 243.
39) A. A. Filippo and M. R. Perrone: IEEE J. Quantum Electron. **28** (1992) 1859.
40) R. A. Mullen, R. C. Lind and G. C. Valley: Opt. Commun. **63** (1987) 123.
41) D. L. Bullock, N.-M. Nguyen-Vo and S. J. Pfeifer: IEEE J. Quantum Electron. **30** (1994) 805.
42) J. Munch, R. F. Wuerker and M. J. LeFebvre: Appl. Opt. **28** (1989) 3099.
43) Y. Kuo, K. Choi and J. K. McIver: Opt. Commun. **80** (1991) 233.
44) V. Kmetik, H. Fiedorowicz, A. A. Andreev, K. J. Witte, H. Daido, H. Fujita, M. Nakatsuka and T. Yamanaka: Appl. Opt. **37** (1998) 7085.
45) A. I. Erokhin, V. I. Kovalev and F. S. Faizullov: Sov. J. Quantum Electron. **16** (1986) 872.
46) R. L. Sutherland: *Handbook of Nonlinear Optics* (Marcel Dekker, New York, 1996) p. 457.
47) F. T. Arecchi and E. O. Schulz-Dubois: *Laser Handbook* (North-Holland, 1972) Vol. 2, p. 1119.
48) A. Yariv: *Quantum Electronics* (John Wiley, New York, 1975) p. 503.
49) D. T. Hon: Opt. Lett. **5** (1980) 516.
50) D. von der Linde, M. Maier and W. Kaiser: Phys. Rev. **178** (1969) 11.
51) H. J. Kong, S. K. Lee and M. Nakatsuka: in preparation.
52) S. K. Lee, D. W. Lee, H. J. Kong and H. Guo: J. Kor. Phys. Soc. **46** (2005) 443.